Inorg. Chem. **2009**, *48*, 3926−3933

Density Functional Analysis of Ancillary Ligand Electronic Contributions to Metal-Mediated Enediyne Cyclization

Aurora E. Clark,*,† Sibaprasad Bhattacharryya,‡ and Jeffrey M. Zaleski*,‡

Department of Chemistry, Washington State University, Pullman, Washington 99164, and Department of Chemistry, Indiana University, Bloomington, Indiana 47405

Received June 17, 2008

Density functional theory (DFT) has been used to study electronic perturbations induced by ancillary halogen ligation within metalloenediyne constructs, and the subsequent affect upon thermal Bergman cyclization temperatures. To isolate electronic from geometric components of Bergman cyclization thermodynamics, model diamine- and diphosphine-enediynes (L = 1,6-diamino- or 1,6-diphosphino-*cis*-1,5-hexadiyne-3-ene) of Mn(II), Cu(II), Zn(II), and Pd(II) with ancillary chloride ligands have been examined computationally and compared to more complex ethylenediamine-based metalloenediyne frameworks of the form MLX_2 (X = Cl, Br, I; L = 1,4-dibenzyl-1,4-diazacyclododec-8-ene-6,10-diyne) with distorted square-planar (Cu(II)), T_d (Zn(II)), and D_{4h} (Pd(II)) geometries. In the latter systems, the ethylenediamine linkage restricts the conformation of the enediyne backbone, causing the alkyne termini separation to be nearly independent of metal geometry (3.75−3.82 Å). Within the Zn(II) family, steric effects are shown to induce conformational changes on the cyclization potential energy surface (PES) prior to the Bergman transition state, introducing distinct electron−electron repulsive interactions. Multiple metal and ligand conformations are also observed on the Cu(II) metalloenediyne cyclization PES. In contrast, square-planar Pd(II) compounds exhibit overlap between the out-of-plane halogen lone pairs and metal d orbitals, as well as the enediyne π system, reminiscent of an organometallic "push−pull" reaction mechanism. These systems have significantly higher predicted activation barriers toward cycloaromatization due to enhanced electron repulsion.

Introduction

The cooperative effects of enediyne geometry and electronic structure upon the thermodynamics of Bergman cyclization have a significant and complicated history in radical chemistry. Generally, the activation barrier for cycloaromatization is related to the terminal alkyne separation, also termed the critical distance cd.[1−4] Given similar geometric structures and cd values, previous work has shown that σ-electron-withdrawing groups at the diyl position increase the cyclization barrier, while donating groups reduce it.[5] In contrast, substitution at the terminal alkyne with σ acceptors or π donors (i.e., halogens) enhances Bergman reactivity by decreasing the activation barrier, while π-withdrawing and σ-donor groups retard cycloaromatization.[6−8] Recent work by Hoffman et al. has broached the possibility of decreasing cd by replacement of the ═CH−, ≡CH, or −C≡ linkages within the enediyne backbone, with isolobal 14 e^- or 15e^- ML_n fragments.[9a] In these hypothetical organometallic complexes, the alkyne termini can be drawn into proximity by engineering C−M−C and M−M−C angles of ∼90°. This compares to more traditional approaches for controlling cd which include linking the terminal alkyne carbons to form cyclic systems. In this latter instance, competitive ring strain can contribute to cyclization thermodynamics,

* Author to whom correspondence should be addressed. E-mail: zaleski@indiana.edu.
† Washington State University.
‡ Indiana University.

(1) Nicolaou, K. C.; Dai, W.-M.; Hong, Y. P.; Baldridge, K. K.; Siegel, J. S.; Tsay, S.-C. *J. Am. Chem. Soc.* **1993**, *115*, 7944.
(2) Nicolaou, K. C.; Ogawa, Y.; Zucarello, G.; Schweiger, E. J.; Kumazawa, T. *J. Am. Chem. Soc.* **1988**, *110*, 4866.
(3) Nicolaou, K. C.; Zucarello, G.; Riemer, C.; Estevez, V. A.; Dai, W.-M. *J. Am. Chem. Soc.* **1992**, *114*, 7360.
(4) Snyder, J. P. *J. Am. Chem. Soc.* **1992**, *112*, 5367.
(5) (a) Jones, G. B.; Warner, P. M. *J. Am. Chem. Soc.* **2001**, *123*, 2134. (b) Jones, G. B.; Plourde, G. W., II. *Org. Lett.* **2000**, *2*, 1757.
(6) Prall, M.; Wittkopp, A.; Fokin, A. A.; Schreiner, P. R. *J. Comput. Chem.* **2001**, *22*, 1605.
(7) Nath, M.; Huffman, J. C.; Zaleski, J. M. *J. Am. Chem. Soc.* **2003**, *125*, 11484.
(8) Semmelhack, M. F.; Gallagher, J. *Tetrahedron Lett.* **1993**, *34*, 4121.
(9) (a) Brzostowska, E. M.; Hoffmann, R.; Parish, C. A. *J. Am. Chem. Soc.* **2007**, *129*, 4401. (b) Schreiner, P. R. *J. Am. Chem. Soc.* **1998**, *120*, 4148. (c) Alabugin, I. V.; Manharan, M. *J. Phys. Chem. A* **2003**, *107*, 3363.

10.1021/ic801117m CCC: $40.75 © 2009 American Chemical Society
Published on Web 08/30/2008

preventing a sound predictive relationship between cd and the activation barrier in some cases.[9b,c] Similarly, enediyne reactivity also can be modulated by chelation to a single metal center. Here, the metal imposes its geometric preference upon the enediyne ligand, thereby dictating cyclization energetics by dynamically altering the ligand ring strain via the terminal alkyne separation.[10] In general, metal coordination of a chelated enediyne ligand alters cyclization reactivity of the free ligand geometrically, rendering thermal reactivity that resembles that of cyclic organic analogues. However, the participation of metal electronic structure and the ability of the metal ancillary ligands to modify Bergman thermodynamics are reaction parameters that have been virtually unexplored. This was highlighted by our preliminary report of conformationally restricted metalloenediynes which exhibit a unique, electronically derived perturbation of the cycloaromatization potential energy surface (PES).[11] There, single-point density functional theory calculations at the crystal structure geometries indicated that the disposition of the ancillary metal ligands may increase the activation barrier for Bergman cyclized products via through-space electronic interactions with the enediyne π system.

In this work, we continue our initial theoretical study and utilize two computational strategies to isolate geometric from electronic contributions to the Bergman cyclization of metalloenediynes. The role of the metal geometry has first been systematically investigated by characterization of the Bergman cyclization PES of $MnLCl_2$, $CuLCl_2$, $ZnLCl_2$, and $PdLCl_2$ metalloenediynes with simple L =1,6-diamino- or 1,6-diphosphino-*cis*-1,5-hexadiyne-3-ene ligands. This test set emphasizes the geometric contribution of the metal to cycloaromatization, while facilitating study of the impact of the ancillary halogen ligands upon cyclization solely via through-bond effects. Experimentally characterized dihalo-(1,4-dibenzyl-1,4-diaza-cyclododec-8-ene-6,10-diyne)M metalloenediynes (M = Zn(II), Cu(II), and Pd(II); X = Cl, Br, and I) also have been examined for comparison.[11,12] Though more computationally intensive, the latter chemical series isolates the electronic contributions of the metal and ancillary halogen ligands because the ethylenediamine unit reduces the ability of the enediyne to adopt conformations in response to changes in metal geometry. The metal geometry does, however, control the structural disposition of the metal−halogen fragment with respect to the enediyne π system, and as a result, a unique relationship is predicted between the cycloaromatization thermodynamics, the relative size of the halogen, and through-space electrostatic interactions between the halogen and the enediyne π framework.

(10) (a) Warner, B. P.; Millar, S. P.; Broene, R. D.; Buchwald, S. L. *Science* **1995**, *269*, 814. (b) Coalter, N. L.; Concolina, T. E.; Streib, W. E.; Hughes, C. G.; Rheingold, A. L.; Zaleski, J. M. *J. Am. Chem. Soc.* *122*, 3112. (c) Schmitt, E. W.; Huffman, J. C.; Zaleski, J. M. *Chem. Comm. 2*, 167.

(11) Bhattacharyya, S.; Clark, A. E.; Pink, M.; Zaleski, J. M. *Chem. Comm.* **2003**, *10*, 1156–1157.

(12) Bhattacharyya, S.; Clark, A. E.; Pink, M.; Zaleski, J. M. *Inorg. Chem.* **2009**, *81*, 3915–3926.

Computational Methods

All geometries were optimized using the Gaussian 98 program,[13] with the unrestricted B3LYP[14] combination of functionals. The 6-31G* basis set[15] was applied to H, C, and N, while the LANL2DZ[16] basis set was used for P (with added diffuse functions),[17] Mn, Cu, Zn, Pd, Cl, Br, and I, with the LANL2 pseudopotential.[16] The basis and pseudopotential for the metal and P atoms takes into account relativistic effects. At the transition metal centers, the high-spin Mn(II) d^5 and Cu(II) d^9 and the closed-shell low-spin Pd(II) d^8 and Zn(II) d^{10} spin states were considered. Spin contamination of the reactant and transition state wave functions was negligible. Calculation of the open-shell, diradical intermediates used the broken-symmetry, broken-spin (BS) approach of Noodleman[18−20] and Yamaguchi, which allows for the α and β electrons to be localized on separate carbon centers.[21] This increased the total molecular $\langle S^2 \rangle$ to near 9.75, 1.75, 1.00, and 1.00, for the Mn(II), Cu(II), Pd(II), and Zn(II) diradical intermediates, respectively. Frequency analyses confirmed that geometries at energetic minima were lacking imaginary vibrations, while transition states were first-order saddle points with a single imaginary vibration corresponding to the reaction coordinate. Thermal and zero-point corrections to the total energy were taken at $T = 298.15$ K, using the harmonic oscillator and frozen rotor approximations.

Model Metalloenediyne Complexes

In this series, *cis*-1,5-hexadiyne-3-ene (**1a**) has been substituted at the alkyne termini positions with amine ($-NH_2$, **2a**) or with phosphine ($-PH_2$, **3a**) functionalities. Neither **2a** nor **3a** has been experimentally prepared; however, they represent simplified models of comparable enediyne ligands and are computationally useful because they lack the structural flexibility imparted by larger systems. The distinguishing feature between the two species lies in the atomic charges at the terminal alkyne carbons and in the relative size of the heteroatom lone pair (LP) orbitals. The $-NH_2$ group is predicted to be slightly electron-withdrawing (by

(13) Frisch, J.; Trucks, G. W.; Schlegel, H. B.; Scuseria, G. E.; Robb, M. A.; Cheeseman, J. R.; Zakrzewski, V. G.; Montgomery, J. A.; Stratmann, R. E.; Burant, J. C.; Dapprich, S.; Millam, J. M.; Daniels, A. D.; Kudin, K. N.; Strain, M. C.; Farkas, O.; Tomasi, J. V.; Barone, V.; Cossi, M.; Cammi, R.; Mennucci, B.; Pomelli, C.; Adamo, C.; Clifford, S.; Ochterski, J.; Petersson, G. A.; Ayala, P. Y.; Cui, Q.; Morokuma, K.; Malick, D. K.; Rabuck, A. D.; Raghavarchari, K.; Foresman, J. B.; Cioslowski, J.; Ortiz, J. V.; Stefanov, B. B.; Liu, G.; Liashenko, A.; Piskorz, P.; Komaromi, I.; Gomberts, R.; Martin, R. L.; Fox, D. J.; Keith, T.; Al-Laham, M. A.; Peng, C. Y.; Nanayakkara, A.; Gonzalez, C.; Challacombe, M.; Gill, P. M. W.; Johnson, B. G.; Chen, W.; Wong, M. W.; Andres, J. L.; Head-Gordon, M.; Replogle, E. S.; Pople, J. A. *Gaussian 98*, revision A.7; Gaussian, Inc.: Pittsburgh, PA, 1998.

(14) Becke, A. D. *Phys. Rev. A: At., Mol., Opt. Phys.* **1988**, *38*, 3098. (a) Lee, C.; Yang, E.; Parr, R. G. *Phys. Rev. B: Condens. Matter Mater. Phys.* **1988**, *37*, 785.

(15) (a) Hehre, W. J.; Ditchfield, R.; Pople, J. A. *J. Chem. Phys.* **1972**, *56*, 2257. (b) Francl, M. M.; Petro, W. J.; Hehre, W. J.; Binkley, J. S.; Gordon, M. S.; DeFrees, D. J.; Pople, J. A. *J. Chem. Phys.* **1982**, *77*, 3654.

(16) (a) Hay, P. J.; Wadt, W. R. *J. Chem. Phys.* **1985**, *82*, 270. (b) Hay, P. J.; Wadt, W. R. *J. Chem. Phys.* **1985**, *82*, 284. (c) Hay, P. J.; Wadt, W. R. *J. Chem. Phys.* **1985**, *82*, 299.

(17) Höllwarth, A.; Böhme, M.; Dapprich, S.; Ehlers, A. W.; Gobbi, A.; Jonas, V.; Köhler, K. F.; Stegmann, R.; Veldkamp, A.; Frenking, G. *Chem. Phys. Lett.* **1993**, *208*, 237.

(18) Noodleman, L. *J. Chem. Phys.* **1981**, *74*, 5737.

(19) Noodleman, L.; Davidson, E. R. *Chem. Phys.* **1986**, *109*, 131.

(20) Noodleman, L.; Norman, J. G., Jr. *J. Chem. Phys.* **1979**, *70*, 4903.

(21) Yamaguchi, K.; Jensen, F.; Dorigo, A.; Houk, K. N. *Chem. Phys. Lett.* **1988**, *149*, 537.

Table 1. UB3LYP/6-31G*/LANL2DZ Thermodynamic Parameters for the Bergman Cyclization of **1a**−**8a** and the Metalloenediyne Retrocyclization Pathways[a]

	$r_{1,6}$	$\Delta H^{\ddagger}$	$\Delta G^{\ddagger}$	$T\Delta S^{\ddagger}$	ΔH_{rxn}	ΔG_{rxn}	$T\Delta S_{rxn}$	$\Delta E_{M=0,1}$
				Cycloaromatization				
1a expt[24,25]	4.32[26]	28			8 ± 3			
1a	4.48	29.9	31.8	−1.9	3.9	6.5	−2.6	
2a	4.54	29.3	33.2	−3.8	4.6	8.7	−4.2	1.1
3a	4.49	38.8	43.2	−4.4	19.3	23.3	−4.0	5.2
4a	3.59	28.9	31.2	−2.2	0.2	2.9	−2.7	1.3
5a	3.58	30.4	31.5	−1.1	3.4	5.6	−1.8	0.9
6a	3.47	27.0	29.5	−2.5	−1.9	1.0	−2.9	1.2
7a	3.50	32.5	33.4	−0.9	12.7	14.1	−1.3	3.8
8a	3.21	26.3	28.3	−2.0	−2.4	−0.3	−2.1	1.4
				Retrocyclization #1				
4b		28.7	28.3	0.5	−0.2	−2.9	2.7	
5b		26.6	25.9	0.7	−3.8	−5.6	1.8	
6b		28.9	28.6	0.4	1.9	−1.0	2.9	
7b		19.8	19.3	0.4	−12.7	−14.1	1.3	
8b		28.7	28.6	0.1	2.4	0.3	2.1	
				Retrocyclization #2				
4b					−3.8	−6.4	2.6	
5b		26.8	26.0	0.9	−4.3	−7.0	2.6	
6b		28.1	27.5	0.6	−3.9	−6.5	2.6	
7b		25.3	24.8	0.5	−2.5	−5.0	2.5	
8b		27.7	27.2	0.6	−4.2	−6.4	2.2	

[a] Vertical singlet triplet energy gaps presented for the benzyne diradical intermediates, $\Delta E_{M=0,1}$. Energy units in kilocalories per mole, terminal alkyne separation $r_{1,6}$ in Å.

0.1 e$^-$ relative to **1a**), while the $-PH_2$ fragment is similarly electron-donating according to Mulliken[22] and Löwdin[23] population analyses. Though the geometries of the reactant, the Bergman transition states (TSs), and diradical intermediates are essentially the same as in the unsubstituted species (see the Supporting Information), the energetic parameters associated with cycloaromatization are perturbed (Table 1). Relative to **1a**, both substituents have increased $\Delta G^{\ddagger}$ and the more endothermic ΔG_{rxn} of reaction due to an increase in LP repulsion along the cyclization coordinate. Due to the significant size of the phosphorus LP orbitals, **3a** has a pronounced increase in $\Delta G^{\ddagger}$ of nearly 10 kcal/mol. In both systems, it is difficult to deconvolve the impact of the electron repulsion between the LP orbitals, which would destabilize the TS and diradical intermediate, and any effect imparted by electron donation or withdrawl at the terminal alkyne carbon. Chelation to a metal center sequesters these LP orbitals in directed bonding, potentially allowing the true impact of electron donation or withdrawl to be assessed (in the absence of ring strain contributions or MX_2 participation in the thermodynamics).

Metalloenediynes **4a**−**6a** are generated by the chelation of **2a** to $MnCl_2$, $CuCl_2$, and $ZnCl_2$ fragments, respectively. Each structure is of C_{2v} symmetry with a Cl−M−Cl σ_v plane. The open-shell Mn(II) d^5 and Cu(II) d^9 centers have slightly squashed tetrahedral geometries with nearly identical alkyne

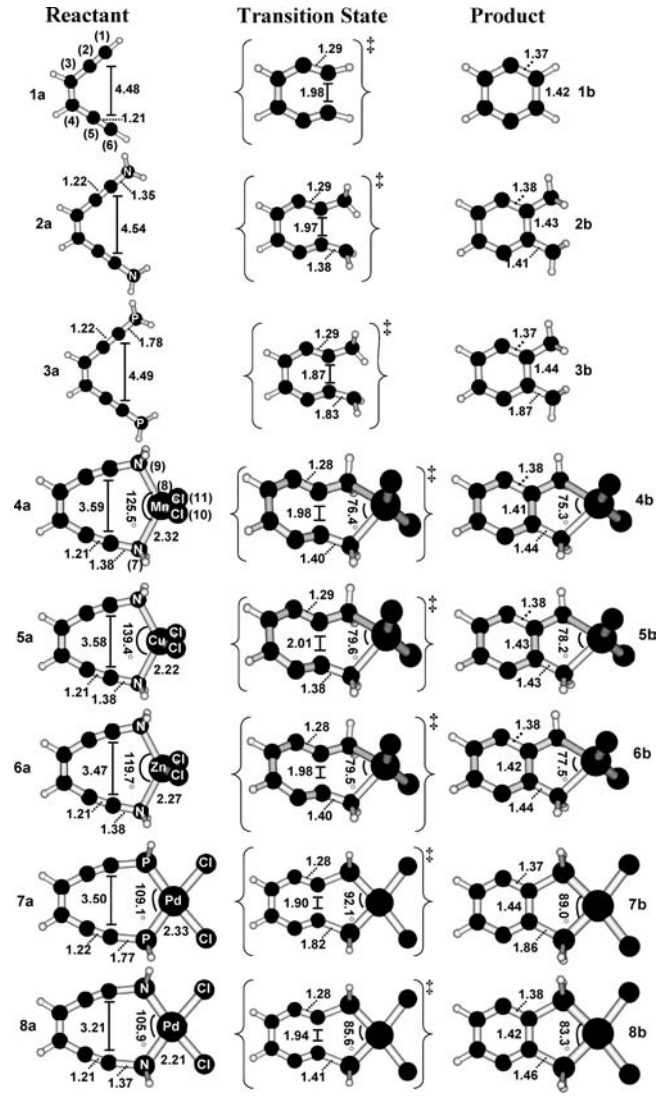

Figure 1. Key structural parameters of the UB3LYP/6-31G*/LANL2DZ optimized enediyne and metalloenediynes **1a**−**8a**, their Bergman cyclization transition states, and the corresponding diradical intermediates **1b**−**8b**.

termini distances ($r_{1,6}$) of ∼3.6 Å. In the closed-shell Zn(II) d^{10} system (**6a**), ideal T_d symmetry about the metal is approached with $r_{1,6}$ = 3.45 Å (Figure 1). The remaining enediyne structural parameters are remarkably similar between the free and chelated ligands, indicating that only $r_{1,6}$ is perturbed by the metal scaffold. The cycloaromatization TSs are characterized by puckering of the developing C1−C6−N7−M8-N9 ring, and the electronic structure of the ligand remains closed-shell, even in the presence of nearby unpaired d electrons. A nonplanar ring structure is similarly observed at the diradical intermediate. A modest (0.4 kcal/mol) trend in the singlet−triplet state splitting of the diradical is observed, ΔE_{ST} **4b** > ΔE_{ST} **5b** > ΔE_{ST} **6b**; however, these values are near that of the free ligand diradical intermediate, indicating only minor interaction between the metal d electrons and the radical centers. These results are in agreement with molecular orbital analyses which suggest that the tetrahedral disposition of the metal and the structural rigidity of the simplified ligand (which forces the metal to lie in the plane of the enediyne) electronically isolate the Mn(II), Cu(II), and Zn(II) centers, validating the structure−

(22) (a) Mulliken, R. S. *J. Chem. Phys.* **1955**, *23*, 1833. (b) Mulliken, R. S. *J. Chem. Phys.* **1955**, *23*, 1841. (c) Mulliken, R. S. *J. Chem. Phys.* **1955**, *23*, 2338. (d) Mulliken, R. S. *J. Chem. Phys.* **1955**, *23*, 2343.
(23) Lowdin, P. O. *Adv. Quantum Chem.* **1970**, *5*, 185.
(24) Wenthold, P. G.; Squires, R. R. *J. Am. Chem. Soc.* **1994**, *116*, 6401.
(25) Davico, G. E.; Bierbaum, V. M.; DePuy, C. H.; Ellison, G. B.; Squires, R. R. *J. Am. Chem. Soc.* **1995**, *117*, 2590.
(26) McMahon, R. J.; Halter, R. L.; Wilson, R. J.; Peebles, S. A.; Kuczkowski, R. L.; Stanton, J. F. *J. Am. Chem. Soc.* **2000**, *122*, 939.

Scheme 1

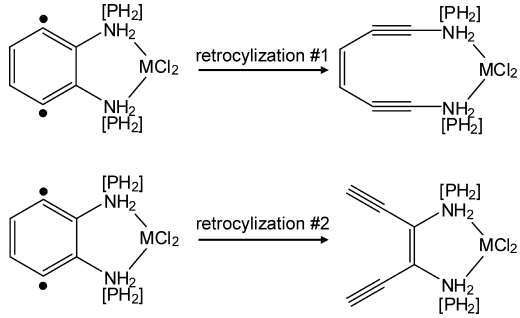

reactivity correlation between the terminal alkyne separation and Bergman cyclization thermodynamics.[1−4] In accordance with the trends in calculated $r_{1,6}$ values, the free-energy order of the activation barriers for Bergman cyclization is **6a** ($\Delta G^{\ddagger}$ = 29.5 kcal/mol) < **4a** ($\Delta G^{\ddagger}$ = 31.2 kcal/mol) ∼ **5a** ($\Delta G^{\ddagger}$ = 31.5 kcal/mol). These values are similar to that observed for a cyclic 10-membered organic enediyne ($\Delta G^{\ddagger}$ = 27.8 kcal/mol, ΔG_{rxn} = 5.2 kcal/mol),[27,28] owing to the comparable separation distances between the alkyne termini ($r_{1,6}$ ∼ 3.39 Å). Note, however, that these activation barriers are within 2 kcal/mol of that of the free ligand. This implies that there is little impact of $r_{1,6}$ upon the thermodynamics until a value of ∼3.5 Å is reached, at which point the energy of the reactant begins to approach that of the TS with decreasing distance between the terminal alkyne carbons. Thus, ring strain contributions to the cyclization thermodynamics are not apparent in these particular tetrahedral systems, and given the electronic isolation of the $-MCl_2$ unit, it is therefore possible to compare the energetics of **1a** and the chelated analogue in order to independently assess the impact of the electron-withdrawing character of the $-NH_2$ unit without LP−LP interactions. Indeed, comparison of the activation barriers for the metal complexes with **1a** indicates that the electron-withdrawing nature of the $-NH_2$ unit does not significantly alter $\Delta G^{\ddagger}$.

In order for the model systems to be relevant to experimental analogues, the Bergman cyclization path under study must be rate-limiting relative to the two potential retrocyclization pathways (Scheme 1), as well as the subsequent H-atom abstraction/addition steps. Investigation of the retrocyclization PES reveals that the DFT activation barriers for ring opening from the diradical intermediate via either path 1 (the microscopic reverse of Bergman cyclization) or path 2 are smaller than the forward cycloaromatization step (Table 1). Further, H-atom abstraction from methane by *para*-benzyne intermediates have reported $\Delta G^{\ddagger}$ values between 10 and 15 kcal/mol.[28,29] Thus, the cycloaromatization path that has been studied for **4a**−**6a** is likely rate-limiting for the reactions that include Bergman cyclization, retrocyclization, and H-atom abstraction steps.

Square-planar metal centers have d_{π} orbitals of the appropriate symmetry to overlap with the enediyne π system and could thus facilitate communication between the metal and ligand. Indeed, benzannulated Pd(II) and Pt(II) metalloenediynes have been prepared with remarkably low Bergman cyclization temperatures (though it has been posited that geometric effects dominated thermodynamics in those cases).[10] We have thus investigated metalloenediynes **7a**−**8a**, which are formed by the chelation of **3a** and **2a** to the $PdCl_2$ fragment, respectively. In **7a**, the long C−PH_2 bond lengths (1.75 Å) decrease the effect of the metal geometry on the enediyne moiety and lead to a $r_{1,6}$ (3.50 Å) that is within 0.05 Å of that observed for similar systems (Figure 1).[10b,c] No spatial overlap is predicted between the Pd d, Cl LP orbitals and enediyne π system (Figure 2), and the ligand electronic structure is unperturbed according to Mulliken or Löwdin population analyses. Though the electron-donating ability of the $-PH_2$ unit is maintained in the metalloenediyne, the absence of P−P LP interactions in the Pd complex decreases the activation barrier by ∼10 kcal/mol ($\Delta G^{\ddagger}$ = 33.4 kcal/mol), and the enthalpy of reaction becomes less endothermic by ∼6 kcal/mol (ΔG_{rxn} =14.0 kcal/mol). Thus, in the absence of any ring strain contributions to the cycloaromatization thermodynamics, it appears that the electron donation of the $-PH_2$ to the terminal alkyne increases the activation barrier by ∼2 kcal/mol.[9]

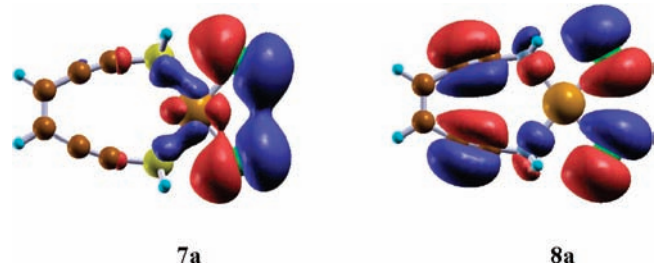

Figure 2. UB3LYP/6−31G*/LANL2DZ highest energy occupied in-plane π MO (α spin) of **7a**−**8a**.

To further explore the energetic consequences of spatial orbital overlap, we have computed the reaction pathway for **8a**, which contains the bidentate diamine enediyne bound to the $PdCl_2$ fragment. Here, short C−N bond lengths ($r_{6,7}$ = 1.37 Å) allow the constricted ligand−metal bond angle to decrease the terminal alkyne separation by 0.3 Å relative to **7a**. Within the frontier MOs, the Cl LP orbitals mix with the in-plane enediyne π system (Figure 2), and significant perturbation of the ligand electronic structure is indicated by the atomic charges. The calculated Mulliken and Löwdin charges are on average 0.4 e^- more positive than **2a** at the bond-forming carbons along the reaction coordinate. Interestingly, $\Delta G^{\ddagger}$ is only ∼3 kcal/mol smaller than that calculated for the Mn(II), Cu(II), and Zn(II) analogues, despite a significant 0.4 Å difference in the distance between the alkyne termini (Table 2). This through-bond electronic effect, arising from the ancillary halogens, is further illustrated by examining the thermodynamics of cyclic 9- and 10-membered enediynes. Here, the $r_{1,6}$ values are calculated to be ∼2.9 Å and ∼3.6 Å, respectively, with $\Delta G^{\ddagger}$ values of ∼16 kcal/mol[27] and ∼28 kcal/mol (BLYP).[28] On the basis of the trend in activation barriers for these cyclic systems,

(27) Schreiner, P. R. *J. Am. Chem. Soc.* **1998**, *120*, 4184.
(28) Koseki, S.; Fujimura, Y.; Hirama, M. *J. Phys. Chem. A* **1999**, *103*, 7672.
(29) Kaneko, T.; Takahashi, M.; Hirama, M. *Tetrahedron Lett.* **1999**, *40*, 2015.

Table 2. B3LYP/6-31G*/LANL2DZ Optimized Geometric Parameters for Compounds **9**−**18**[a]

	$r_{1,6}$	$\alpha_{1,2,3}$	$\omega_{8,9,10,11}$	$r_{12,14}$	$r_{12,13}$	$\alpha_{13,12,14}$
9a	4.00 (3.90)	175.1	170.9			
9‡	1.91	134.2	63.1			
9b	1.44	127.7	63.1			
10a T_d $ZnCl_2$	3.80 (3.78)	171.5	60.4	2.28	2.35	121.3
10i	3.79	171.5	64.1	2.28	2.36	121.2
10‡	1.90	132.7	0.0	2.31	2.32	133.4
10b	1.43	128.8	0.1	2.33	2.31	133.2
11a T_d $ZnBr_2$	3.80 (3.74)	174.4	60.7	2.52	2.45	119.3
11i	3.78	174.3	65.6	2.53	2.44	119.9
11‡	1.90	132.7	0.0	2.48	2.47	131.2
11b	1.43	127.5	0.0	2.50	2.47	131.4
12a T_d ZnI_2	3.79	174.2	61.7	2.72	2.64	116.8
12i	3.47	168.7	40.1	2.70	2.66	126.8
12‡	1.90	132.7	0.0	2.68	2.66	128.2
12b	1.43	127.4	0.0	2.69	2.66	127.8
13a D_{4h}-*ps* $CuCl_2$	3.81 (3.76)	174.4	51.1	2.40	2.39	93.2
13i T_d $CuCl_2$	3.79	173.7	62.5	2.24	2.29	134.0
13‡	1.88	134.9	50.1	2.39	2.39	91.9
13b	1.44	129.5	32.3	2.39	2.39	91.6
14a D_{4h}-*ps* $CuBr_2$	3.82 (3.88)	174.6	52.8	2.53	2.53	91.0
14i T_d $CuBr_2$	3.91	173.4	52.8	2.44	2.47	94.8
14‡	1.88	134.8	52.2	2.53	2.53	90.0
14b	1.44	129.5	48.4	2.53	2.53	85.6
15a D_{4h}-*ps* CuI_2	3.83	174.6	54.5	2.69	2.68	89.2
15i T_d CuI_2	3.87	174.1	56.0	2.63	2.66	90.6
15‡	1.88	134.9	53.1	2.68	2.68	88.5
15b	1.44	129.5	50.2	2.68	2.68	88.3
16a D_{4h} $PdCl_2$	3.81 (3.82)	171.6	51.9	2.31	2.31	96.5
16i	3.79	171.3	62.5	2.24	2.29	134.0
16‡	1.91	132.7	29.4	2.30	2.29	97.7
16b	1.43	127.9	0.2	2.26	2.29	146.9
17a D_{4h} $PdBr_2$	3.82 (3.88)	172.0	53.1	2.47	2.48	93.2
17i	3.91	173.9	52.8	2.47	2.44	94.8
17‡	2.01	137.8	53.2	2.49	2.44	93.8
17b	1.43	130.3	50.2	2.49	2.42	94.5
18a D_{4h} PdI_2	3.83 (3.86)	172.1	54.8	2.68	2.68	89.7
18i	3.87	172.7	56.0	2.66	2.63	90.6
18‡	1.89	133.9	53.4	2.70	2.61	90.6
18b	1.43	130.3	50.1	2.68	2.61	91.9

[a] The local geometry of the metal center presented: T_d = tetrahedral, D_{4h}-*ps* = distorted square planar, D_{4h} = square planar. Available experimental values in parentheses.[12] Bond lengths, terminal alkyne separation ($r_{1,6}$) in Å, angles α and dihedrals ω in degrees.

the $\Delta G^{\ddagger}$ for **8a** would be anticipated to be 3−4 kcal/mol smaller than our calculated value.

Examination of the retrocyclization pathways of **7b** indicate a small free energy of activation along path 1 (Scheme 1, Table 1). This barrier is similar to what would be predicted for H-atom abstraction by the diradical intermediate and may indeed lead to the abstraction event becoming rate-limiting. For our purposes, however, **7a** merely serves to illustrate that the forward cyclization is more favored than in the free ligand and that the long distance between the metal and the terminal alkyne carbons inhibits any electronic effect from the ancillary Cl LP orbitals. Importantly, **8a** exhibits energetics for the two retrocyclization pathways that ensure that the forward cycloaromatization studied is rate-limiting and that the electronic influence exhibited by ancillary halogen ligands justifies further study using computationally intensive and experimentally viable constucts.

Ethylenediamine-Based Metalloenediyne Complexes

The synthesis and reactivity of the ligand (L) 1,4-dibenzyl-1,4-diaza-cyclododec-8-ene-6,10-diyne (**9a**) and its CuX_2, ZnX_2, and PdX_2 (X = Cl, Br, I) complexes are discussed in a companion manuscript (Figure 3).[12] The most notable feature of the metalloenediyne complexes is that the bidentate, ethylenediamine unit constrains the ligand such that the terminal alkyne separation and enediyne conformation are nearly independent of the structural preference of the metal. Comparison of a series of MLX_2 compounds (M = Cu(II), Zn(II), Pd(II)) indicates large deviations in the temperatures for Bergman cyclization using differential scanning calorimetry (DSC). The ethylenediamine further poises the metal above the plane of the enediyne, facilitating an electronic perturbation whose energetic consequences may be inferred from observations that the distorted square-planar Cu(II) dihalogen complexes have Bergman cyclization temperatures that only modestly depend upon X, while the tetrahedral Zn complexes show marked dependence upon the ancillary halogen ligand.[12]

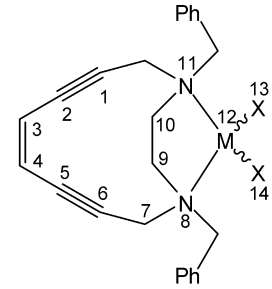

10a (M=Zn, X=Cl) **13a** (M=Cu, X=Cl) **16a** (M=Pd, X=Cl)
11a (M=Zn, X=Br) **14a** (M=Cu, X=Br) **17a** (M=Pd, X=Br)
12a (M=Zn, X=I) **15a** (M=Cu, X=I) **18a** (M=Pd, X=I)

Figure 3. Ethylenediamine-based metalloenediyne complexes, with numbering scheme (Ph = phenyl).

An X-ray structure and DFT calculations of ligand **9a** reveal that the ethylenediamine linkage in the free ligand adopts a trans conformation (Table 2). The enediyne backbone lies perpendicular to the ethylenediamine plane, and thus the alkyne termini are forced to a separation distance ($r_{1,6}$) of 4.00 Å (3.90 Å exptl). The DFT cycloaromatization TS is characterized by the constriction of $\alpha_{1,2,3}$, which forces the ethylenediamine to rotate to an approximate *cis* conformation and lie below the plane of the enediyne framework, a conformation that is retained in the diradical intermediate **9b**. The calculated free energy of activation is 37.9 kcal/mol, while ΔG_{rxn} is 16.9 kcal/mol (Table 3). The entropic cost of the trans to cis rotation is minimal, such that $T\Delta S^{\ddagger}$ is −1.1 kcal/mol and $T\Delta S_{rxn}$ is −2.0 kcal/mol. Although this reaction is predicted to be endothermic, the two subsequent H-atom abstraction steps drive the reaction, and cyclized products have been characterized.[12] DSC reveals an exotherm associated with Bergman cyclization at 170 °C (Table 3).

In the first series of ethylenediamine-based metalloenediynes, **9a** is chelated to the following metal fragments: $ZnCl_2$ to form **10a**, $ZnBr_2$ to form **11a**, and ZnI_2 to form **12a**. Here, ligand chelation and the d^{10} electronic configuration of the Zn(II) lead to a tetrahedral disposition of the N_2Cl_2 ligand set about the metal core. As a consequence of chelation, the ethylenediamine bridge adopts an approximate *cis* conformation ($\omega_{8,9,10,11} \sim 60°$), which is also reflected in the X-ray structures of these compounds. The relative rigidity of the

Table 3. UB3LYP Thermodynamic Parameters for the Bergman Cyclization of **9a**−**18a**, the syn → anti Rotation of the Phenyl Rings in the Zn(II) Complexes **10a**−**12a**, and the Transformation of Local Metal Geometries in the Cu(II) Complexes, **13** − **15** (D_{4h}-*ps* = distorted square planar; T_d = tetrahedral)[a]

	$r_{1,6}$	DSC °C[12]	$\Delta H^{\ddagger}$	$\Delta G^{\ddagger}$	$T\Delta S^{\ddagger}$	ΔH_{rxn}	ΔG_{rxn}	$T\Delta S_{rxn}$	$\Delta E_{M=0,1}{}^{v}$	$\Delta E_{M=0,1}{}^{ad298}$
9a	4.0	170	36.9	37.9	−1.1	14.9	16.9	−2.0	2.1	
10i	3.79	207	38.5	39.2	−0.7	13.9	14.9	−1.0	1.6	1.3
11i	3.78	154	37.1	37.8	0.7	12.8	14.3	−1.5	2.2	1.3
12i	3.47	144	28.3	29.5	−1.2	4.3	6.9	−2.6	1.7	1.2
13i	3.79	141	39.1	41.0	−1.9	12.2	15.2	−3.1	1.0	0.9
14i	3.91	144	42.6	43.7	−1.1	18.8	19.9	−1.0	0.1	0.01
15i	3.90	NA	46.3	47.1	−0.7	19.8	21.6	−1.8	0.4	0.02
16a	3.81	226	51.7	51.6	−0.04	24.9	25.6	−0.1	1.3	0.9
17a	3.82	212	53.8	52.2	−0.4	25.0	25.8	−0.8	0.9	0.9
18a	3.83	196	52.1	52.4	−0.4	25.2	25.9	−0.7	1.0	0.9
10a → **10i**						0.7	0.6	0.1		
11a → **11i**						1.6	1.8	−0.2		
12a → **12i**						10.2	9.3	0.9		
13a (D_{4h}-*ps*) → **13i** (T_d)						11.3	9.4	1.9		
14a (D_{4h}-*ps*) →**14i** (T_d)						5.9	4.9	1.0		
15a (D_{4h}-*ps*) →**15i** (T_d)						5.5	3.5	2.0		

[a] Vertical and adiabatic (corrected for ZPE and 298 K) singlet−triplet energy gaps for the metallobenzynes, $\Delta E_{M=0,1}{}^{v}$, and $\Delta E_{M=0,1}{}^{ad298}$ also presented. Energy units in kilocalories per mole, terminal alkyne separation, $r_{1,6}$, in Ångstroms.

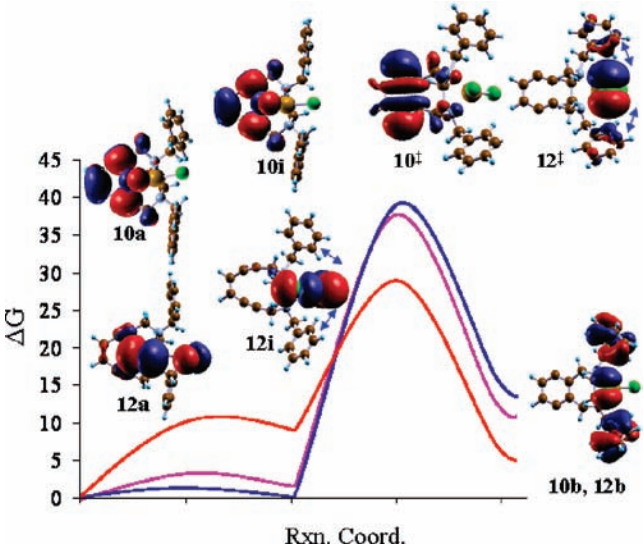

Figure 4. HOMOs of the starting reactant, intermediate, Bergman cyclization TS, and *para*-benzyne diradical intermediate for compounds **10** (blue), **11** (purple), and **12** (red). The associated free-energy differences, ΔG, in kilocalories per mole.

ligand is highlighted by the minor ∼0.2 Å decrease in terminal alkyne separation upon the chelation of **9a** to ZnX_2 (Table 2), which agrees well with the 0.1−0.16 Å experimental range. Thus, the general conformation of the enediyne ligand and metal center is essentially identical for the dichloride, dibromide, and diiodide complexes. Further, the ethylenediamine bridge causes one of the ancillary halogen ligands to lie directly above the plane of the enediyne ligand, and the C_1−C_6 Bergman cyclization reaction coordinate. When X = Cl, the halogen is 3.28 Å above the center of the 1,5-hexadiyne unit, $r_{13,z}$,[30] and "through-space" interactions are observed between the Cl LP and enediyne π orbitals (Figure 4, **10a** and **12a**) causing a disparity in calculated Zn−Cl bond lengths ($r_{12,13}$ = 2.28 Å: $r_{12,14}$ = 2.35 Å) in agreement with the X-ray structure.[12] A systematic increase in $r_{13,z}$ is observed from 3.28 Å in **10a** to 3.42 Å in **11a** to 3.60 Å in **12a**, although the disparity in Zn−X bond lengths persists along the series owing to a commensurate increase in the size of the halogen LP orbitals (Table 2).

The cyclization TSs of the dihalogen compounds are characterized by conformations of both of the phenyl rings that are syn relative to the metal (Figure 4). This is in contrast to the experimental and DFT reactant conformations, which have one ring syn and one anti. Initially, we proposed that the phenyl ring rotation was induced by the closing benzyne ring; however, after further investigation, it appears that, for steric reasons, both phenyl rings must be pointing away from the ligand in order to reach the TS. This is confirmed by the optimized intermediate structures **10i**−**12i**, which have both phenyl rings in a syn conformation about the metal and lie 0.68, 1.83, and 6.83 kcal/mol above the global reactant minima, respectively. The TSs associated with rotation were not successfully optimized; however, since the relative energies of the intermediates increase going down group VII, the respective activation barriers for the conformational change also likely follow the trend $ZnLCl_2$ < $ZnLBr_2$ < $ZnLI_2$. Electron repulsion between the halogen LP and the phenyl rings is one explanation for the disparate energies of the intermediate structures. In the cases of **10i** and **11i**, the interaction is end-on (LP-σ) with the phenyl H atoms, which are ∼2.5 Å from halogen atom 14. In contrast, **12i** exhibits a LP interaction with the phenyl π system because the rings are oriented parallel to the ancillary iodide (Figure 4, inset). This repulsive interaction is combined with a significant 0.3 Å decrease in the alkyne termini separation relative to **10i**−**11i**, leading to a net increase in the relative energy of the diiodide intermediate.

Intrinsic reaction coordinate calculations (IRC) confirm that the Bergman cyclization TSs are approached from the conformational intermediates **10i**−**12i**. In general, the Bergman TS geometry is characterized by the rotation of the ZnX_2 unit away from the enediyne ligand as the ethylenediamine bridge rotates from $\omega_{8,9,10,11} \sim 60°$ to $\sim 0°$. The net result is an increase in the distance between the halogen and enediyne plane, which precludes any "through-space" interaction

(30) This distance was determined by considering the right triangle formed by Cl13, C6, and a point along the C1−C6 line such that: $r_{13,x} = r_{13,6}$ (sin $\alpha_{1,6,13}$).

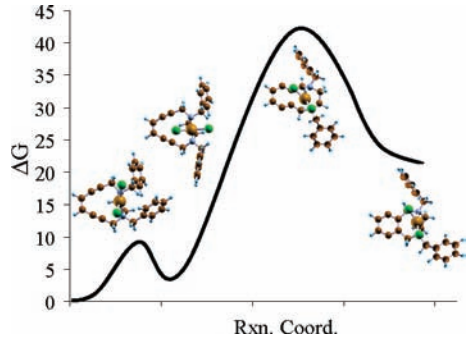

Figure 5. Free-energy differences, ΔG (kcal/mol), of structures along the Bergman cyclization PES of **13**.

between the halogen and the enediyne π orbitals (Figure 4) and causes equivalent Zn−X bond lengths at the TS. Interestingly, the energy differences between the starting reactants **10a**−**12a** and the cycloaromatization TSs (**10**‡−**12**‡) are all nearly identical (39.2, 38.7, and 38.5 kcal/mol, respectively), while the activation barriers from the intermediates **10i**−**12i** exhibit a large variation: **10i**, $\Delta G^{\ddagger} = 39.2$; **11i**, $\Delta G^{\ddagger} = 37.8$; **12i**, $\Delta G^{\ddagger} = 29.5$ kcal/mol. Thus, the thermodynamic trend in activation barriers as the intermediates (**10i**−**12i**) go to the Bergman TSs (**10**‡−**12**‡) is considered to be due to the varying degrees of destabilization at the intermediate structures (Figure 4).

At the diradical intermediate, the benzyne ligand has nearly identical structural parameters along the halogen series, and no "through-space" interaction is observed between the metal−halogen unit and the ligand. The trend in reaction energetics (**10i**, $\Delta G_{rxn} = 14.9$ kcal/mol; **11i**, $\Delta G_{rxn} = 14.3$ kcal/mol; **12i**, $\Delta G_{rxn} = 6.9$ kcal/mol) qualitatively agrees with that of the experimental DSC temperatures associated with the Bergman cyclization of **10a**−**12a** (Table 3) and may be attributed to differences in the relative energies of the pretransition state intermediates (Figure 4). The observed DSC temperature of **10a** is 207 °C, while that of **11a** is 154 °C, and that of **12a** is 144 °C. Thus, the net 60 °C variation in DSC temperatures across the Zn halogen series appears to correlate to a ∼10 kcal/mol difference in the computed free energies of activation.

DFT calculations on the $CuLX_2$ (X = Cl, Br, I) metalloenediyne complexes of **9a**, labeled **13a**−**15a**, respectively, reveal that the Cu(II) metal center adopts a distorted square-planar geometry that is common to four-coordinate *cis*-CuN_2Cl_2 structures (Figure 5).[31] Generally, the predicted geometries are somewhat closer to being square-planar than in the X-ray structure; however, the structural rigidity of the ethylenediamine backbone facilitates good agreement between the theoretical and experimental values for the terminal alkyne separation.[12] The approximate square-planar disposition of the Cu(II) center places the halogens above the $-NH_2$ groups of the ethylendiamine bridge, leading to enediyne π orbitals that are unperturbed relative to the free ligand. Metal−halogen bond lengths increase going down group VII, but the M−X bond lengths are equivalent in each complex. Thus, no structural or electronic trends are observed in the Cu(II) metalloenediyne reactants that would form a basis for deviations in Bergman reactivity in this series. Interestingly, the computed vibrational data for the square-planar reactants indicate low energy modes that correspond to distortion of the Cu(II) center toward a tetrahedral geometry. This prompted us to initiate the geometry optimization of the Cu(II) reactants with T_d metal centers in order to assess the structural stability of tetrahedral Cu(II) reactants. The analysis resulted in the optimization of approximately tetrahedral MLX_2 intermediates **13i**−**15i**, which are further characterized by rotation of one of the phenyl groups such that one ring is *syn* and the other *anti* relative to the metal. The dichloride T_d intermediate is 9.4 kcal/mol higher in energy than the square-planar isomer, while the dibromide and diiodide intermediates are 4.9 and 3.5 kcal/mol higher in energy, respectively.

Following the cyclization paths from the tetrahedral intermediates leads to Bergman TSs that are characterized by distorted square-planar metal centers, but that have the same phenyl group rotation. IRC calculation connects **13i**−**15i** with the distorted square-planar Bergman TSs (**13**‡−**15**‡) having free energies of activation of 41.0, 42.6, and 46.3 kcal/mol, respectively. The modest increase in $\Delta G^{\ddagger}$ along the Cu(II) halogen series may be attributed to two factors. Going down group VII, the energies of the near T_d intermediate structures sequentially decrease relative to the distorted square-planar reactants. Presuming that the relative energies of the TSs are constant, this would increase the activation energy along the halogen series. Second, a 0.1 Å increase in alkyne termini separation is observed at the intermediate structures, which should stabilize the pseudo-T_d intermediates relative to the more distorted, square-planar TS structures. These data qualitatively agree with the experimental trend in DSC cyclization temperatures for **13a**−**14a**, which exhibit exothermic peaks at 141 and 144 °C, respectively. Unfortunately, the diiodide analogue was not able to be prepared experimentally, and DSC data are unavailable.

The diradical Bergman product of the $CuLCl_2$ compound is characterized by a pseudo square-planar metal center,[32] while the $CuLBr_2$ and $CuLI_2$ diradical intermediates have local metal geometries that are near T_d. Variations in the metal conformation do not affect the free energies of reaction from **13i**−**15i**, which have only a 5 kcal/mol deviation along the halogen series: $\Delta G_{rxn} = 15.2$, 19.9, and 21.6 kcal/mol, respectively.

In contrast to the T_d metal geometry of the Zn(II) complexes, which have been found to induce "through-space" interactions between the enediyne π and halogen LP orbitals, and the distorted square-planar geometry of the Cu(II) metalloenediynes, which have relatively no electronic influence upon the enediyne ligand, the square-planar Pd(II) center investigated in the final metalloenediyne series has the potential to participate in "through-bond" interactions with the ligand owing to the symmetry and size of the metal d orbitals. Here, **9a** is chelated to fragment $PdLCl_2$ to form

(31) Benites, P. J.; Rawat, D. S.; Zaleski, J. M. *J. Am. Chem. Soc.* **2000**, *122*, 7208–7217.

(32) It should be noted that a second cycloaromatization PES was found that had a syn configuration of the phenyl rings relative to the metal center. However, this cyclization path had a higher activation barrier and more endothermic reaction energy than the path that had an anti conformation of the phenyl units. Interestingly, the *syn* conformation leads to a Cu(II) metal geometry that is truly tetrahedral, while the anti favors a pseudo-T_d metal center.

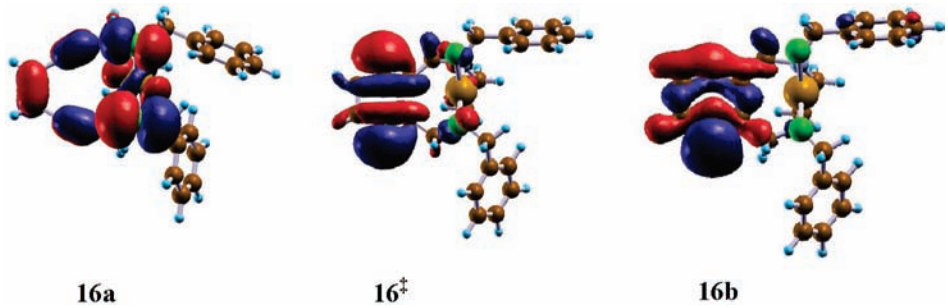

Figure 6. Highest occupied ligand-centered α orbitals of **16a**−**16b**.

16a, $PdBr_2$ to form **17a**, and $PdLI_2$ to form **18a**. The reactant geometries are in good agreement with the X-ray structure,[12] having deviations in bond lengths by 0.01 Å and in bond angles by 1−2°. The phenyl rings adopt similar conformations to the Zn(II) analogues; however, the square-planar disposition of the metal above the plane of the enediyne causes the halogens to be oriented on either side of the ligand, rather than pointing directly above the enediyne π system. The size and symmetry of the Pd d orbitals, as well as the disposition of the halogen ligands, facilitate mixing of the halogen LP and metal d orbitals with the localized enediyne π orbitals, as seen in Figure 6. This orbital description is reminiscent of the organometallic "push−pull" mechanism of the model metalloenediyne **8a** and has similar dramatic consequences on the energetics of cycloaromatization for the series of Pd analogues.

The transition states **16**‡−**18**‡ notably have the same phenyl ring conformation as the reactant, with one ring *syn* and one anti relative to the metal center. IRC analysis confirms that the Bergman cyclization TSs are directly connected to **16a**−**18a**, with no intermediate structures present on the PES. The ligand TS conformation is similar to that of the Zn(II) transition states discussed previously, with the exception of slightly smaller $r_{1,6}$ values and ethylenediamine bridges that maintain an approximate *cis* conformation with $\omega_{8,9,10,11} \sim 50°$ instead of $\sim 0°$. Importantly, the TS molecular orbitals do not exhibit mixing of halogen LP and metal d orbitals because the localized frontier orbitals of the enediyne TS are σ in nature and not π (Figure 6). The electronic isolation of the $PdLX_2$ unit is maintained at the diradical cycloaromatized products **16b**−**18b**, whose ligand conformations are nearly identical to the Zn(II) systems, with the exception of the dihedral angle of the ethylenediamine unit.

Since the starting geometric parameters of the ligand along the PES are most similar to those of the Zn(II) complexes discussed above, the distinctive "through-bond" π delocalization in the Pd(II) reactants is likely responsible for the ∼10 kcal/mol increase in activation energy relative to **10a**−**12a**. A similar argument may be invoked for the free energy of reaction, which is ∼10 kcal/mol more endothermic than in the Zn(II) derivatives. The "through-bond" nature of the electronic perturbation appears to have a larger influence upon Bergman cyclization thermodynamics than the "through-space" interaction observed in the Zn(II) halide series. This computational result qualitatively agrees with the experimental DSC temperatures associated with Bergman cyclization, wherein the Pd(II) compounds have significantly higher DSC temperatures than the Zn(II) metalloenediynes. The Pd(II) metalloenediyne temperatures range from 196° to 226°, while the Zn(II) metalloenediyne temperatures range from 144° to 207°. We also note that the relatively constant DSC values for the Pd(II) halogen series are reflected in the nearly identical values for the free energy of activation. This is in contrast to the ∼60° variation in the DSC temperatures in the Zn(II) halogen series, which corresponds to a ∼10 kcal/mol difference in the computed activation barriers.

Conclusion

In order to isolate electronic from geometric components of Bergman cyclization thermodynamics, model diamine− and diphosphine−enediyne Mn(II), Cu(II), Zn(II), and Pd(II) dichloride compounds have been examined, in addition to more complex ethylenediamine-based metalloenediynes MLX_2 (X = Cl, Br, I) of distorted square-planar (Cu(II)), tetrahedral (Zn(II)), and square-planar (Pd(II)) geometries. Within the simplest metalloenediyne constructs, the tetrahedral systems were found to be electronically isolated from the enediyne ligand. Here, thermodynamic trends were most similar to organic nine-membered ring systems. In contrast, the ancillary halogens of the Pd(II) compounds were found to alter the energetics of cycloaromatization via a "through-bond" mechanism. Through-bond electronic perturbation of the enediyne ligand by ancillary halogen ligands was also observed in the ethylenediamine-based $PdLX_2$ systems. In both cases significant increases in cyclization activation barriers were observed. The conformational flexibility of the ethylenediamine−enediyne ligand further allowed for through-space interactions between the ancillary halogen ligands and the enediyne π framework (e.g., $ZnLX_2$ compounds). Here, modulation of the distance between the halogen and the enediyne moiety led to distinct trends in activation barriers along the dichloride, dibromide, and diiodide series. Conformational changes within the phenyl ring orientations also introduced steric and electronic repulsive interactions at the Bergman cyclization TS, increasing the activation barrier for the Zn(II) compounds as a set, relative to their Cu(II) analogues.

Acknowledgment. AEC thanks Ernest R. Davidson for thoughtful discussions.

Supporting Information Available: Cartesian coordinates of all compounds. This material is available free of charge via the Internet at http://pubs.acs.org.

IC801117M